Available online at www.sciencedirect.com
ScienceDirect
Ceramics International 34 (2008) 279–284
CERAMICS INTERNATIONAL
www.elsevier.com/locate/ceramint

PM304 coating on a Ni-based superalloy rod for high temperature lubrication

C.H. Ding *, P.L. Li, G. Ran, J.N. Zhou

State Key Laboratory for Mechanical Behavior of Materials, Xi'an Jiaotong University, Xi'an, Shaanxi 710049, PR China

Received 21 April 2006; received in revised form 17 July 2006; accepted 21 September 2006
Available online 13 November 2006

Abstract

PM304 coating on a Ni-based superalloy rod for high temperature lubrication has been prepared by high-energy ball milling and powder metallurgy techniques. The composition of the PM304 coating is the same as that of PS304 coating, but the microstructure is quite different. The microstructure of PM304 coating is fine and dense; the size of self-lubricating particles in the coating is very small. Self-lubricating Cr_2O_3 particles are about 100 nm, BaF_2/CaF_2 particles about 1 μm, Ag particles below 5 μm, while BaF_2/CaF_2 and Ag particles precipitated from NiCr matrix are less than 50 nm. The fine and dense microstructure results in increased tensile strength and crack growth resistance of PM304 coating. The mean tensile strength is about 46 MPa.
© 2006 Elsevier Ltd and Techna Group S.r.l. All rights reserved.

Keywords: Milling; Sintering; Composites

1. Introduction

Above 540 °C, conventional solid lubricants, such as graphite and Cr_3C_2, are unacceptable for application because of their inadequate oxidation resistance. PS304 coating developed by NASA Glenn (previous NASA Lewis) Research Center is a plasma spray deposited coating for the reduction of friction and wear in turbomachinery applications [1,2]. PS304 consists of a Ni80Cr20 matrix and three solid lubricants: Cr_2O_3 (20 wt.%), Ag (10 wt.%) and eutectic BaF_2/CaF_2 (10 wt.%). NiCr matrix acts as a binder and offers excellent high temperature oxidation/corrosion resistance and essential mechanical strength. Cr_2O_3 functions as both a hardener and a high temperature lubricant when the temperature is above 500 °C [3], BaF_2/CaF_2 offers effective lubrication above 400 °C. Ag acts as a thermochemically stable solid lubricant at a relatively lower temperature range, i.e. from room temperature to approximately 450 °C. Plasma-sprayed coatings consist of flat plate-like lamella, and the true contact only occupies a portion, sometimes even less than 25%, of the apparent interlamellar contact [4]. This results in the porous microstructure (15 vol.% porosity) and the low cohesive strength (less than 35 MPa). Furthermore, volume shrinkage and residual stresses due to the thermal expansion mismatch and to the effect of plastic deformation introduce cracks in the coatings after plasma spraying [5]. The existence of interconnected porosity and segmented cracks in PS304 coatings not only affects the mechanical properties, but also deteriorated the wear resistance of the coatings.

Powder metallurgy is a convenient method to prepare bulk components with fine and dense microstructure, quality control is relatively simple, for example, the final composition is the same as the starting powders, in contrast to the plasma spraying technique where some components may be lost in the deposition process [6]. PM304 bushing, made only via powder metallurgy using PS304 powder with the size range of 40–110 μm as starting material, was reported. But, till data, no literature on PM304 coating or its microstructure is reported. The high-energy ball milling technique is an effective method for producing nanostructured composite powders for metal matrix composites (MMCs) [7]. In the milling process, deformation, breaking and cold welding of powder particles is continuously repeated, leading to mechanical alloying of particles. For a ductile/brittle material combination such as NiCr and Cr_2O_3, BaF_2/CaF_2, the particles of the brittle powder will be broken into fine particles in the process, embedded or

* Corresponding author. Tel.: +86 29 8266 9791; fax: +86 29 8323 7910.
E-mail address: chding@mail.xjtu.edu.cn (C.H. Ding).

0272-8842/$34.00 © 2006 Elsevier Ltd and Techna Group S.r.l. All rights reserved.
doi:10.1016/j.ceramint.2006.09.016

dissolved into the matrix. A composite powder with a refined structure is thereby produced. The mechanical properties and wear resistance of MMCs strongly depend on the amount, size and distribution of hard phases in the metal matrix [7,8]. So in this work, high-energy ball milling and powder metallurgy are applied to prepare PM304 coating with fine and dense microstructure on a Ni-based superalloy rod.

2. Experimental procedure

The starting material was commercial Ni/Cr (80/20, 60% in weight percent, or wt.), Cr_2O_3 (20 wt.%), Ag (10 wt.%) and eutectic BaF_2/CaF_2 (62/38, 10 wt.%) powder in the size range of 50–100 μm. Cr_2O_3 and eutectic BaF_2/CaF_2 powders were first put into a Simoloyer ball mill for milling for 5 h, then Ni/Cr and Ag powders were added into the mill for milling, the total milling time was 20 h. The ratio of ball to powder was 10:1 in weight. The powders were milled in Ar gas at a rotational speed of 1000 rpm in a stainless steel chamber using age-hardened 17%Cr stainless steel balls with diameter of 6 mm. The total powder charge was 100 g. After being milled the powder was examined by X-ray diffraction (XRD), scanning electron microscopy (SEM) and energy dispersion spectroscope (EDS). A Ni-base superalloy rod with diameter 19 mm was undercut with depth 0.35 mm. Cold isostatic pressing (CIP) method was used to press the powder into the undercutting surface of the rod under the pressure of 500 MPa. Between the powder and the undercutting surface there was a very thin interlayer (the thickness about 0.05 mm) of Ag, Cr (35 wt.%) and Cu (3 wt.%) powders as solder. Then the rod was sintered in a vacuum furnace at 1100 °C for 2 h. After being sintered, the polished cross-section of PM304 coating was examined by XRD, SEM and TEM. In order to measure the tensile strength of PM304 coating, the same Ni-base superalloy rod with diameter 16 mm was undercut to form a columned hole (Ø 12 × 1.0) on the top plane of the rod. The Ag, Cr (35 wt.%) and Cu (3 wt.%) powders were first put into the hole, then the milled powder was added into the hole followed by cold isostatic pressing at 500 MPa. Subsequently, the specimen was sintered at 1100 °C for 2 h. After being sintered, the rod was ground to remove the cylinder of Ni-based superalloy and form a rod with diameter 10 mm. Fig. 1 schematically shows how the specimen is prepared. The top plane of PM304 was ground, then glued to the plane of stainless steel rod using a two-part epoxy. The specimens were cured in air for 100 h. Tensile test was carried out by INSTRON-4466 machine at the strain rate of $1 \times 10^{-4}\,S^{-1}$. The density of the sintered samples was determined by Archimede's method, using alcohol as the medium of immersion. The PS304 coatings were deposited onto Ni-based superalloy substrate. The starting powder was in the size range of 40–110 μm. The deposition procedures were fully described in Ref. [9].

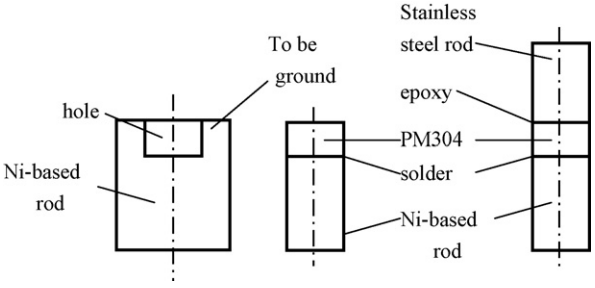

Fig. 1. The schematic figure of the specimen.

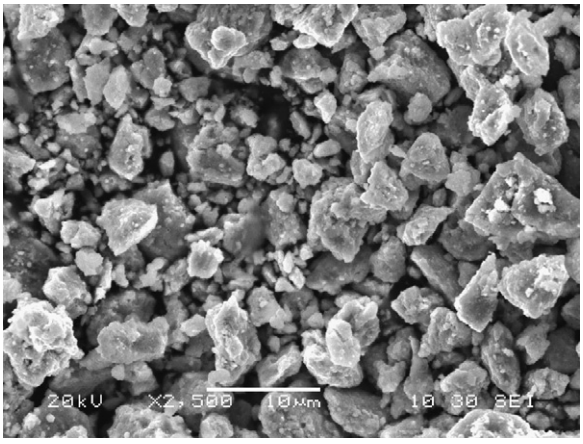

Fig. 2. SEM image of PM304 powders after 20 h milling.

3. Results and discussion

Fig. 2 presents the morphology of the powder after milling for 20 h. It shows that after 20 h milling, the particles are fine, and the size of particles is less than 10 μm. EDS analysis indicates that most of particles contain the elements as expected.

Fig. 3 shows XRD patterns of original and milled powder as well as sintered coating. It was noted that the peaks of NiCr and Cr_2O_3 became broader and the intensity weaker with increasing milling time because of the refinement of the grains and increasing atomic level strain. After milling for 20 h, the grain size of Cr_2O_3 became about 20 nm on the basis

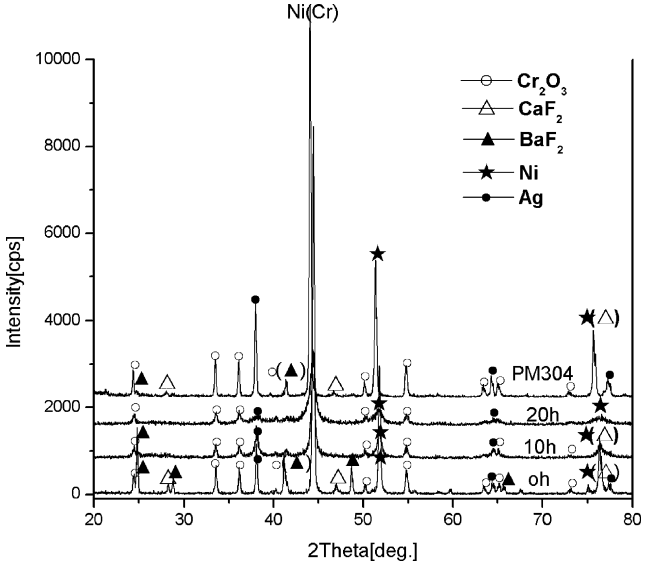

Fig. 3. XRD patterns for PS304 powders and sintered coating.

of the Scherrer equation, few peaks of BaF_2/CaF_2 could be detected, and some peaks of Ag disappeared. The reason is that some BaF_2/CaF_2 and Ag dissolve or cut into NiCr and Cr_2O_3 particles, and the amorphization and internal stress of these phases can also cause their peaks to become weaker, broad or disappeared. After sintering at 1100 °C for 2 h, the diffraction peaks of PM304 coating became almost the same as those of original powders, demonstrating that the dissolved or embedded BaF_2/CaF_2 and Ag precipitated or floated from NiCr matrix and Cr_2O_3 particles during sintering process. Furthermore, none of the reactants between the components of PM304 was detected. This indicates that the PM304 material can be employed in high temperature environment requiring thermal stability.

Fig. 4 presents PM304 coating on a Ni-based superalloy rod: (a) PM304 coating on the rod after CIP and sintering and (b) PM304 coating after ground. Fig. 4a shows that after CIP and sintering obviously latitudinal shrinkage of PM304 coating can be observed, indicating that densification of the coating occurred during CIP and sintering. Fig. 4b shows that PM304 coating on the Ni-based superalloy rod has been successfully prepared by powder metallurgy technique.

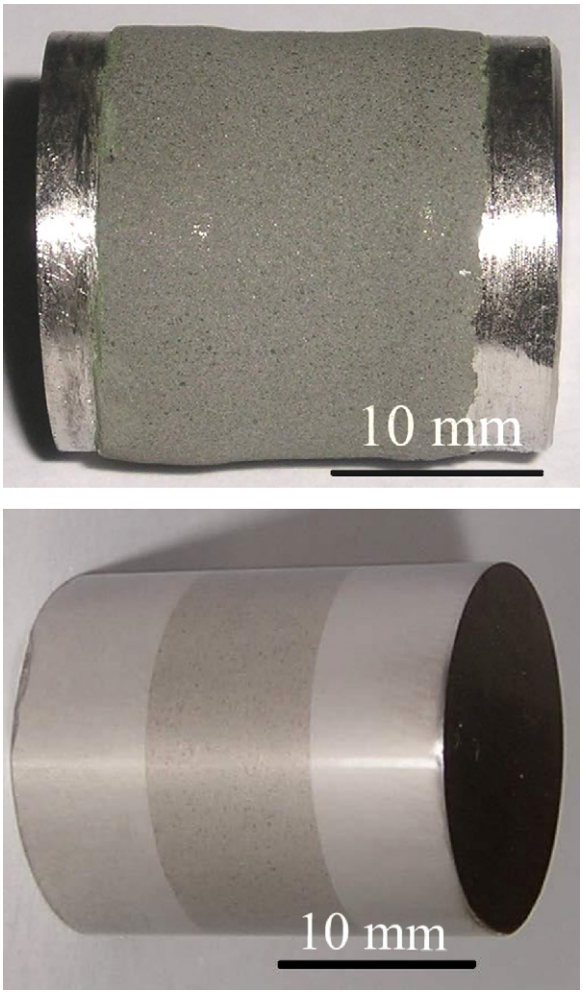

Fig. 4. PM304 coating on a Ni-based superalloy rod after CIP and sintering (a) and after ground (b).

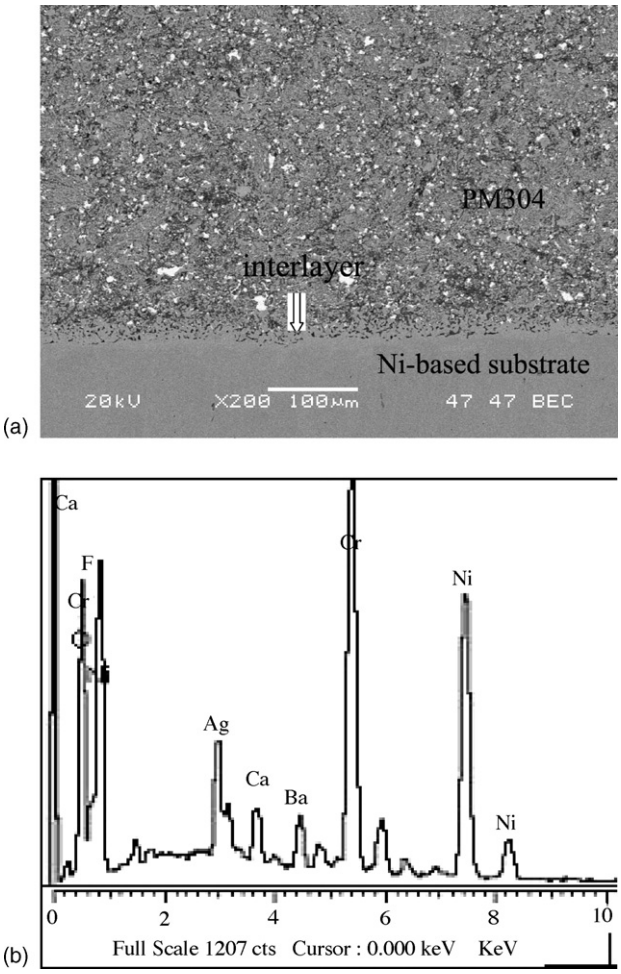

Fig. 5. SEM back-scattered image (a) and EDS spectra (b) of PM304 coating.

The microstructure and EDS spectra of PM304 sintered at 1100 °C for 2 h are shown in Fig. 5. It can be observed from Fig. 5a that the microstructure is dense, and is quite different from that of PS304 coating comprised of laminar and coarse phases. The relative density of PM304 is 0.93 (absolute density is 7.7 g/cm^3), higher than that of PS304 (about 0.85). EDS spectra (Fig. 5b) indicates that elements designed exist in the PM304 coating. Between the PM304 coating and the Ni based substrate there was a thin interlayer of Ag, Cr (35 wt.%) and Cu (3 wt.%). It can be seen that a good bond was obtained with the interlayer by powder metallurgy under this experimental condition. However, there were several long cracks between the PS304 coating and Ni based substrate, even the length of a crack over 50 μm [10].

Fig. 6 is a magnified micrograph of Fig. 5a showing that there are three types of phases, i.e. the white, deep gray and gray phase, as marked by A, B and C, respectively. EDS analysis indicates that the white phase is rich in Ag (80–90 wt.%), the deep gray phase is rich in Cr (30–40 wt.%), O (10–20 wt.%), Ba (5–15 wt.%), F (5–15 wt.%), Ca (3–10 wt.%), while the gray phase is rich in Ni (80–85 wt.%), Cr (15–20 wt.%) and contain a few Ag, F, Ba, Ca, O. In the present case, it can be seen that the self-lubricating phases are composite phase. For example, Ag-rich phases contain 2–3 wt.% Ba, 2–3 wt.% Ca, 4–5 wt.% F,

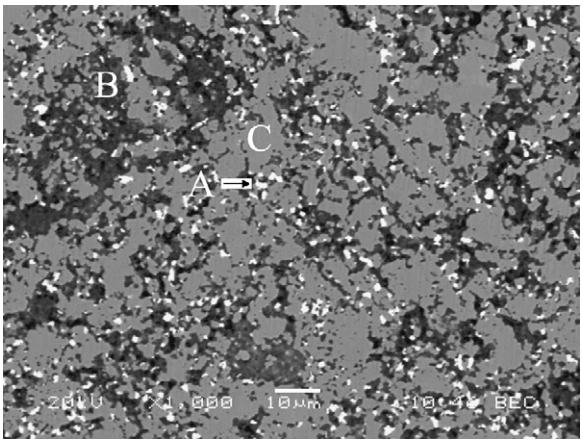

Fig. 6. A magnified SEM back-scattered micrograph of Fig. 5(a).

and the deep gray phases contain 3–5 wt.% Ni and about 1–2 wt.% Ag.

Fig. 7 is a more magnified micrograph of Fig. 6 showing that the deep gray phases consist of small black particles. Many of the particles are about 100 nm, with some of them rather about 1 μm. EDS shows that the small particles with a size on nano-scale are Cr_2O_3. Since grain size of Cr_2O_3 particles is about 20 nm after milled and the melting point of Cr_2O_3 (2400 °C) is very high, the growth rate of Cr_2O_3 phase is slow during sintering at 1100 °C for 2 h, which leads to the existence of nanostructured Cr_2O_3 particles. The big particles are BaF_2/CaF_2 phase precipitated or floated from Cr_2O_3 particles that grew up during sintering because the melting point of eutectic BaF_2/CaF_2 is only 1020 °C. The white particles are Ag phase with a grain size less than 5 μm. On the gray (NiCr) phase, there are some small black particles with a size less than 1 μm. Fig. 8a is a TEM image showing that the particles are less than 50 nm and a selected area diffraction pattern and its index for particles (Fig. 8b) proves that they are BaF_2/CaF_2 and Ag particles. However, in PS304 coatings, the size of Cr_2O_3 and eutectic BaF_2/CaF_2 phases was about 5–10 μm and the length of Ag flaks over 15 μm [2]. As compared with PS304 coating, the size of self-lubricating particles in PM304 coating is much smaller.

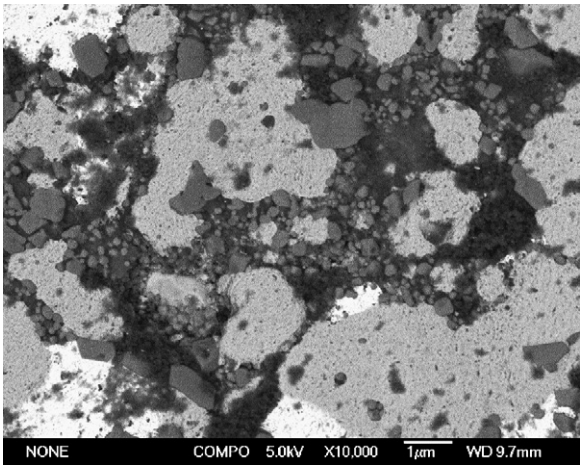

Fig. 7. SEM back-scattered micrograph of PM304 coating.

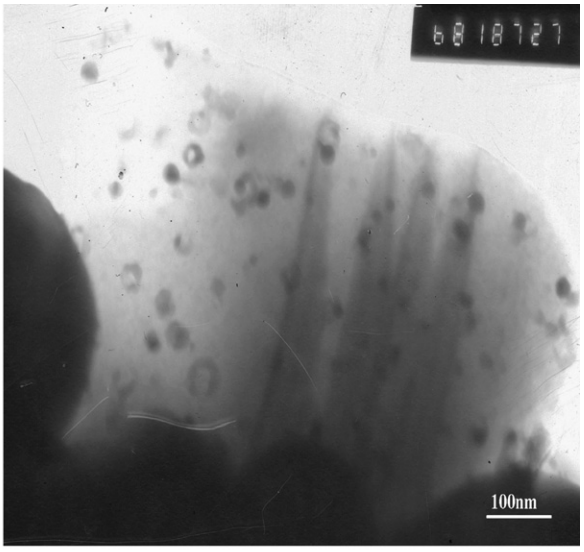

(a)

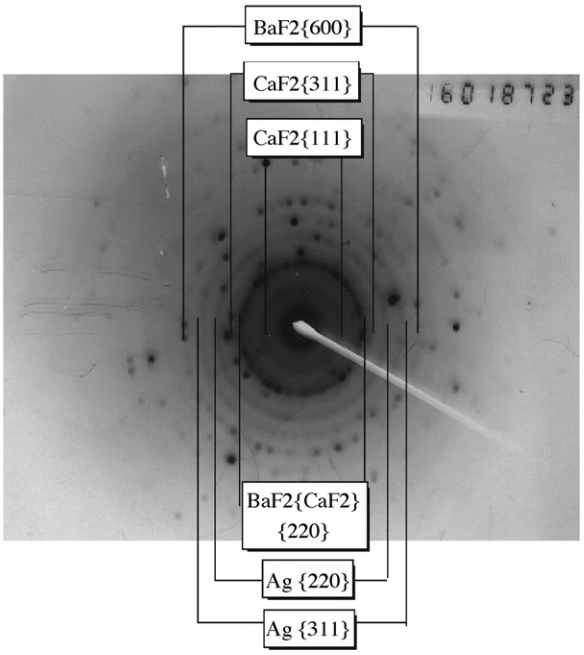

(b)

Fig. 8. TEM image (a), selected area diffraction pattern and its index (b) for self-lubricating particles in PM304.

The mean tensile strength of PM304 coating was about 46 MPa and all fracture during tensile test occurred inside the body of the coating (cohesive failure). It was anticipated that NiCr matrix was likely to dominate the strength of PS304 coatings [4]. However, the yielding strength of NiCr alloy is greater than 220 MPa, much exceeds the maximum tensile strength of PS304 coating (35 MPa) [5]. So the NiCr matrix could not dominate the maximum tensile strength of PS304 coating. In fact, PS304 coating contains 30 wt.% ceramic phases (Cr_2O_3 20 wt.% and BaF_2/CaF_2 10 wt.%) and high porosity (15 vol.%), it is the ceramic phases that result in a low tensile strength, while the high porosity deteriorates the strength further. But, in PM304 coating, the porosity is low (7 vol.%) and the self-lubricating phases are fine. As a result, eliminating porosity and refining ceramic phases can enhance

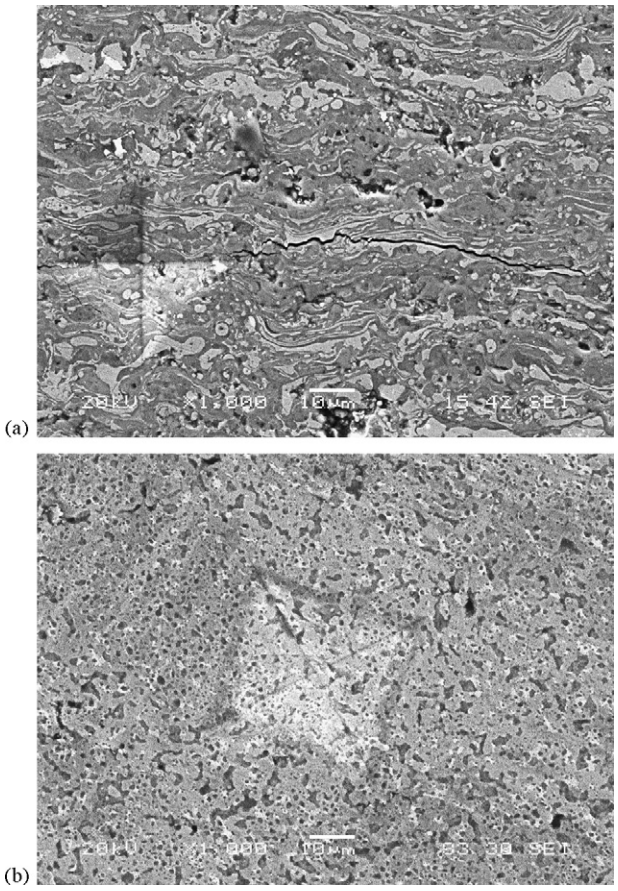

Fig. 9. SEM micrographs of the indents of PS304 (a) and PM304 (b).

the inter-particle adhesion, which inhibit inter-particle cracking and delay the occurrence of interfacial failure, resulting in increased tensile strength [11].

Fig. 9 shows the SEM micrographs of the indents on the surface of PS304 and PM304 coatings at the load of 4.9 N. Comparing Fig. 9a with b, it can be seen that the long crack appeared on the surface of PS304 after the identation. Since a limited real contact between the rapidly solidifying splats could weaken the grain boundary strength [4] it was thought that cracks would propagate along areas of weakness under cyclic stress [12]. The crack preferentially propagates in the direction parallel to the substrate surface on the surface of PS304. Furthermore, the residual tensile stress resulting from the anisotropy of elastic and thermal expansion properties could also weaken the grain boundary [13] with an important effect on the cohesive strength of the thermal sprayed coatings [14]. However, the stresses could be relaxed by plastic deformation. With grain size decreasing, the plasticity of particles increased because the grain boundary diffusion was enhanced by the high concentration of grain boundaries [15]. In PM304 coating, more plastic deformation provided a process for more energy dissipation and reduced the stresses due to the decrease of grain size, which resulted in high cohesive strength between splats and in few cracks appeared on the surface of PM304 after the identification. Additionally, owing to the presence of splat boundaries, the crack length measured could not be used to calculate the fracture toughness of the coatings. However, the crack length was affected by the crack growth resistance of the coating. The higher the crack growth resistance of the coating, the shorter the crack length [16]. Thus, with smaller grains, higher density and higher cohesive strength PM304 composite is expected to have better crack growth resistance than that of PS304.

4. Conclusions

PM304 coating on a Ni-based superalloy rod can be prepared by high-energy ball milling and powder metallurgy techniques. The microstructure of PM304 coating was dense, the size of self-lubricating particles was small. Cr_2O_3 particles were about 100 nm, BaF_2/CaF_2 particles about 1 μm, Ag particles below 5 μm, while BaF_2/CaF_2 and Ag particles precipitated from NiCr matrix were less than 50 nm. The PM304 coating exhibited relative density of 0.93. The refinement of self-lubricating phases and increase of the relative density resulted in increased tensile strength and crack growth resistance of PM304; the mean tensile strength was about 46 MPa.

Acknowledgements

The authors wish to thank the National Science Foundation of China (Grant No. 50471033) for providing financial support for this work.

References

[1] C. Dellacorte, B.J. Edmonds, Preliminary Evaluation of PS300: A New Self-Lubricating High Temperature Composite Coating for Use to 800 °C, NASA TM-107056, 1995.
[2] W.C. Wang, Application of a high temperature self-lubricating composite coating on steam turbine components, Surf. Coat. Technol. 177–178 (2004) 12–17.
[3] G.H. Liu, F. Rubbevalloire, J. Blovet, Improvement in tribological properties of chrome oxide coating at high temperature by solid lubricants, Wear 160 (1993) 181–189.
[4] C. Li, A. Ohmori, R. McPherson, The relationship between microstructure and Young's modulus of thermally sprayed ceramic coatings, J. Mater. Sci. 32 (1997) 997–1004.
[5] D.R. Mumm, A.G. Evans, I.T. Spitsberg, Characterization of a cyclic displacement instability for a thermally grown oxide in a thermal barrier system, Acta Mater. 49 (2001) 2329–2340.
[6] C. DellaCorte, H.E. Sliney, Tribological Properties of PM212: A High Temperature, Self-Lubricating, Powder Metallurgy Composite, NASA-TM-102355, 1990.
[7] I.S. Polkin, A.B. Borzov, F.H. Froes, C. Suryanarayana, in: Proceedings of the Second International Conference on Structural. Applications of Mechanical Alloying, Vancouver, Canada, September 20–22, (1993), pp. 157–164.
[8] J. He, M. Ice, E.J. Lavernia, Synthesis and characterization of nanostructured Cr_3C_2–NiCr, Nanostruct. Mater. 10 (8) (1999) 1271–1283.
[9] C. Dellacorte, The effect of counterface on the tribological performance of a high temperature solid lubricant composite from 25 to 650 °C, Surf. Coat. Technol. 86–87 (1996) 486–492.
[10] C. DellaCorte, V. Lukaszewicz, M.J. Valco, K.C. Radil, H. Heshmat, Performance and Durability of High Temperature Foil Air Bearings for Oil-Free Turbomachinery, NASA/TM-209187, 2000.

[11] X.Y. Qin, S.H. Cheong, Tensile behavior of nanocrystalline Ni–Fe alloy, Mater. Sci. Eng. A363 (2003) 62–66.
[12] A. Skopp, M. Woydt, K.H. Habig, Unlubricated sliding friction and wear of various Si3N4 pairs between 22 and 1000 °C, Tribol. Int. 23 (1990) 189–199.
[13] S. Cho, B.J. Hockey, B.R. Lawn, S.J. Bennison, Grain size and R-curve effects in abrasive wear of alumina, J. Am. Ceram. Soc. 72 (1989) 1249–1252.
[14] R. McPherson, The relationship between the mechanism of formation, microstructure and properties of plasma-sprayed coatings, Thin Solid Film 83 (1981) 297–310.
[15] A.S. Edelstein, J.S. Murday, B.B. Rath, Challenges in nanomaterials design, Prog. Mater. Sci. 42 (1997) 5–12.
[16] H. Luo, D. Goberman, L. Shaw, M. Gell, Indentation fracture behavior of plasma sprayed nanostructured Al_2O_3–13 wt.% TiO_2 coatings, Mater. Sci. Eng. A 346 (2003) 237–245.